



# OPEN Protective effects of *Rosa roxburghii* Tratt. extract against UVB-induced inflammaging through inhibiting the IL-17 pathway

Shuhong Zhang<sup>1,3</sup>, Yueyue Chen<sup>1,3</sup> & Liping Qu<sup>1,2,3</sup>✉

Chronic inflammation is a critical mechanism contributing to the aging process; however, research specifically addressing chronic inflammation in skin biology remains limited. This study investigates the protective mechanism of *Rosa roxburghii* Tratt. (RRT) extract against UVB-induced inflammaging. RRT extract effectively reduces the secretion of IL-6, IL-1 $\alpha$ , TNF- $\alpha$ , and PGE2 in keratinocytes. Additionally, it attenuates UVB-induced IL-17 pathway activation by downregulating IL-17RA, c-Fos, and c-Jun protein levels, as well as the gene expression of IL-17RA, TRAF6, HSP90, and IKK $\gamma$ . Co-culturing human foreskin fibroblasts (HFF) with inflammatory factors secreted by UVB-exposed keratinocytes reveals that these factors significantly reduce mitochondrial membrane potential and mitochondrial reactive oxygen species (ROS), thereby promoting aging in HFF. The anti-inflammaging effects of RRT extract are achieved through the reduction of  $\beta$ -galactosidase activity, targeting of the TGF- $\beta$ 1-Smad2/3 signaling pathway, upregulation of COL1A1 expression, and reduction of senescence-associated secretory phenotype secretion. This study provides a novel perspective and robust scientific foundation for exploring mechanisms of skin aging and potential therapeutic interventions.

**Keywords** Inflammaging, Inflammatory factors, Keratinocytes, Human foreskin fibroblasts, IL-17 signal pathway, *Rosa. roxburghii* Tratt.

The concept of “inflammaging,” first introduced by Franceschi et al. in 2000, emphasizes the persistent presence of low-level chronic inflammation associated with aging<sup>1</sup>. This is characterized by elevated serum levels of proinflammatory factors and a shift toward cellular senescence<sup>2,3</sup>. Chronic inflammation has been recognized as one of the 12 hallmarks of aging, which accelerates the aging process through various mechanisms and causes cumulative damage to tissues and organs over time<sup>4</sup>. During aging, senescent cells accumulate in the skin and secrete a senescence-associated secretory phenotype (SASP), exacerbating chronic inflammation<sup>5</sup>. The interplay between cell senescence, inflammation, and decline in skin function may establish a self-perpetuating cycle that intensifies progressively. Consequently, the protective functions of the skin, which are designed to provide defense, gradually become compromised and undermined by inflammatory mechanisms<sup>6</sup>. Despite the acknowledged significance of inflammaging in skin aging, research on its precise mechanism of action remains limited.

The skin, which is the largest organ of the body, consists of two primary layers: the epidermis and dermis. The epidermis is primarily composed of keratinocytes and keratin proteins that serve as crucial protective barriers. Within the dermis, fibroblasts, collagen, and elastic fibers form an essential framework for maintaining the skin structure and elasticity<sup>6,7</sup>. Chronic inflammation associated with skin aging is influenced by various factors, including UV radiation<sup>8</sup>. UV radiation, particularly UVB (280–315 nm), infiltrates the skin and damages cellular mitochondria and DNA, thereby contributing to a spectrum of skin injuries<sup>9</sup>. This damage triggers sustained inflammatory responses by promoting the release of inflammatory mediators and activating multiple inflammatory pathways<sup>10,11</sup>. The IL-17 signaling pathway has been implicated in the regulation of these inflammatory processes, underscoring its pivotal role in immune homeostasis and host defence mechanisms<sup>12</sup>.

<sup>1</sup>Yunnan Botanee Bio-Technology Group Co., Ltd., Yunnan 650106, China. <sup>2</sup>Yunnan Characteristic Plant Extraction Laboratory, Yunnan Yunke Characteristic Plant Extraction Laboratory Co., Ltd., Yunnan 650106, China. <sup>3</sup>Shanghai Jiyan Biomedical Development Co., Ltd., Shanghai 201702, China. ✉email: quliping@botanee.com

The IL-17 family, which includes IL-17A–E, plays a pivotal role in immune responses by binding to specific receptor complexes such as IL-17RA and IL-17RC<sup>13</sup>. The activation of these receptors initiates downstream signaling pathways (such as ERK, JNK, and p38), within target cells, leading to the transcription and release of various proinflammatory factors<sup>14,15</sup>. Despite the increasing interest in skin aging research, studies on how UVB-induced inflammation in the epidermis affects aging in the dermis remain relatively limited.

*Rosa. roxburghii* Tratt. (RRT), an indigenous wild resource of the Yunnan-Guizhou Plateau and western Sichuan Plateau<sup>16</sup>, is extensively used in traditional folk medicine across China to treat enteritis and dysentery, promote digestion, and strengthen the spleen<sup>17</sup>. RRT is known for its abundant bioactive compounds, including polyphenols and flavonoids, as well as particularly high levels of ascorbic acid<sup>18</sup>. It exhibits several physiological functions such as immune regulation, antioxidant activity, anti-apoptotic properties, and anti-aging effects<sup>19,20</sup>. However, the scientific literature on its specific benefits against inflammaging and modulation of the IL-17 signaling pathway remains limited.

The objective of this study was to explore the cellular responses of human foreskin fibroblasts (HFF) to the accumulation of inflammatory factors released by keratinocytes and to investigate the protective effects of the RRT extract against inflammaging. We elucidated that inflammatory factors induce the aging process by paracrine action, and RRT extract demonstrated a significant anti-inflammatory effect through the IL-17 signaling pathway. This approach is expected to provide new insights into the mechanism of skin aging.

## Results

### Target compounds characterized from RRT fruit extract

Based on high-performance liquid chromatography (HPLC) analysis, Fig. 1a presents the chromatogram of the RRT extract, highlighting a distinct peak. By comparing the retention time of the RRT extract (1.126 min) with that of the standard ascorbic acid sample, and corroborating the ultraviolet absorption at 245 nm, it was confirmed that the primary component of the RRT fruit extract is ascorbic acid (Fig. 1b), aligning with findings from previous studies<sup>18</sup>. Quantitative analysis, performed using a standard calibration curve, revealed that the concentration of ascorbic acid in the RRT fruit extract was  $1.80 \pm 0.17\%$ .

### RRT extract mitigated UVB-induced keratinocytes damage

To investigate the potential protective effects of the RRT extract against UVB radiation, an initial cytotoxicity assessment was conducted. As illustrated in Fig. 2a, the viability of keratinocytes exceeded 90% following treatment with varying concentrations of RRT extract (ranging 15.6–500  $\mu\text{g/mL}$ ), suggesting that the RRT extract is non-toxic at concentrations up to 500  $\mu\text{g/mL}$ . Figure 2b presents a flowchart detailing the processing of keratinocytes with UVB radiation and the RRT extract. As illustrated in Fig. 2c, the control group cells exhibit normal morphology and robust growth. In contrast, cells exposed to UVB radiation exhibited significant morphological alterations, including cell death and abnormal morphology, as indicated by the red arrows in the figure. Treatment with RRT at concentrations of 50, 100, and 200  $\mu\text{g/mL}$  resulted in a marked decrease in cellular damage, with substantial recovery observed in both cell morphology and growth. Quantitative analysis revealed that UVB irradiation (30  $\text{mJ/cm}^2$ ) resulted in a significant reduction in keratinocyte viability compared to the control group, with a mortality rate of 28.9%. However, treatment with RRT extract significantly mitigated UVB-induced cell damage ( $P < 0.01$ ). Furthermore, the protective effect against UVB-induced damage was positively correlated with the concentration of the RRT extract.

### RRT extract alleviated the inflammatory response induced by UVB in keratinocytes

Upon exposure to UVB irradiation, keratinocytes showed a marked increase in the secretion of inflammatory factors ( $P < 0.01$ ). Specifically, the secretion of IL-6 surged to 525.85  $\text{pg/mL}$ , corresponding to an 8.15-fold

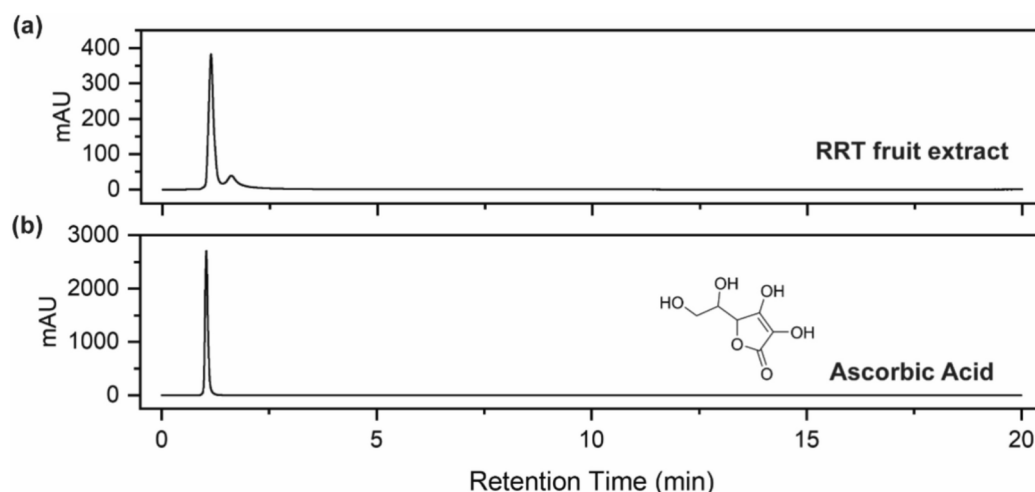


**Fig. 1.** Characterization of target compounds in RRT fruit extract. (a) HPLC chromatogram of the RRT fruit extract. (b) HPLC chromatogram of the ascorbic acid standard.

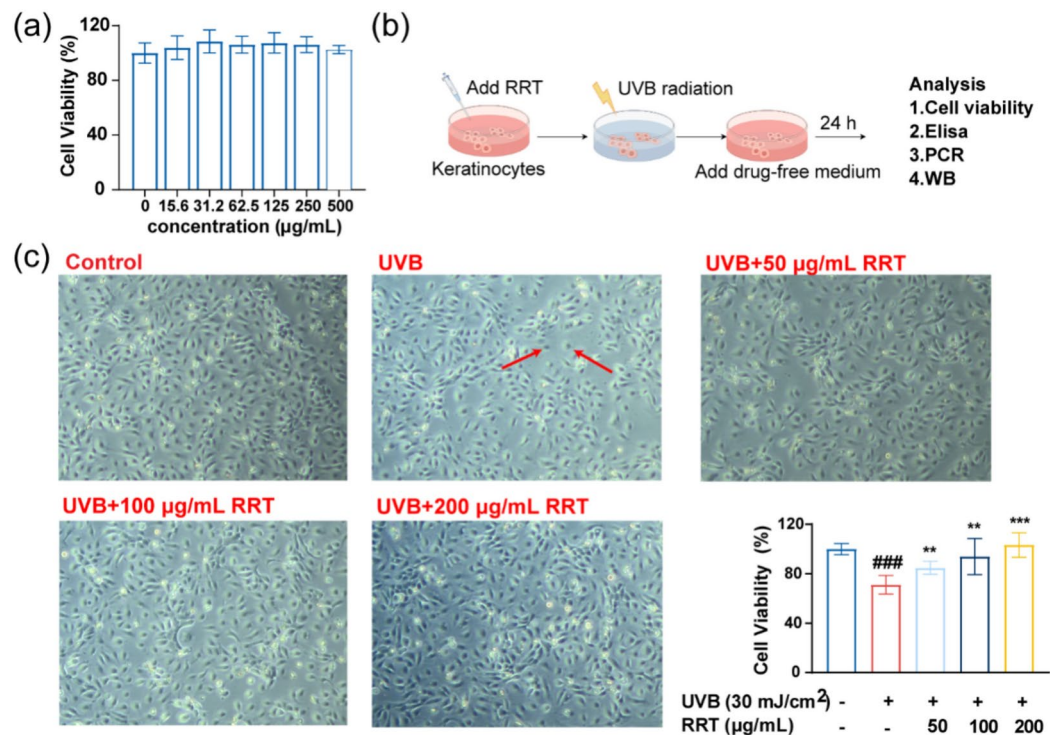


**Fig. 2.** Viability of keratinocytes under UVB irradiation and RRT extract treatment. **(a)** Keratinocyte viability after 24-h treatment with varying concentrations of RRT extract. **(b)** Flow chart of keratinocytes with UVB and RRT extract processing. **(c)** Morphological (magnification: ×20) and viability assessments of keratinocytes after UVB radiation and RRT extract treatment. Statistical analysis involved one-way ANOVA and paired two-tailed t-tests, with significance denoted as ### $P < 0.001$ , \*\* $P < 0.01$ , \* $P < 0.05$  relative to the control group, and \*\*\* $P < 0.001$ , \*\* $P < 0.01$ , \* $P < 0.05$  relative to the control group.

increase relative to that in the non-irradiated control group (Fig. 3a). In addition, IL-1 $\alpha$  secretion rose by 1.49-fold, reaching 26.52 pg/mL (Fig. 3b), TNF- $\alpha$  secretion escalated by 5.33-fold to 72.55 pg/mL (Fig. 3c), and PGE2 secretion experienced a 13.8-fold increase, attaining a concentration of 776.65 pg/mL (Fig. 3d). These findings highlighted the significant proinflammatory effects of UVB irradiation on keratinocytes. Notably, treatment with RRT extract at a concentration of 200 µg/mL significantly led to a reduction in the secretion levels of IL-6 ( $P < 0.001$ ), IL-1 $\alpha$  ( $P < 0.05$ ), TNF- $\alpha$  ( $P < 0.001$ ), and PGE2 ( $P < 0.001$ ) when compared to the UVB-exposed group. This indicates the potential anti-inflammatory effect of RRT extract in mitigating UVB-induced inflammatory responses in keratinocytes. Moreover, a concentration-dependent inhibition of TNF- $\alpha$  secretion by RRT extract was observed, with significant reductions evident at concentrations as low as 50 µg/mL.

### RRT extract suppresses IL-17 pathway on UVB-induced keratinocytes

As illustrated in Fig. 4a, UVB irradiation resulted in a significant upregulation of IL-17RA, HSP90, TRAF6, IKK $\gamma$ , MMP1, MMP3 gene expression levels in keratinocytes compared to the control group ( $P < 0.001$ ). These genes were annotated within the genetic regulatory pathways in the Kyoto Encyclopedia of Genes and Genomes (KEGG) database, with particular emphasis on the IL-17 regulatory pathway (<https://www.genome.jp/kegg/>). Figure 4b show that UVB irradiation led to a significant 2.03-fold increase in IL-17RA protein expression. In addition, UVB exposure markedly increased the expression of the inflammatory proteins c-Jun and c-Fos ( $P < 0.001$ ), which are critical downstream effectors of the IL-17 pathway. This upregulation signifies activation of the IL-17 pathway. Treatment with RRT extract resulted in a significant reduction in the expression of these genes and proteins, with the highest concentration of RRT extract (200 µg/mL) exhibiting the most notable suppression. These results indicate that the RRT extract exerts anti-inflammatory effects by inhibiting the IL-17 pathway. Furthermore, the expression of MMP1 and MMP3 markedly increased following UVB irradiation in keratinocytes, with MMP3 showing a particularly significant upregulation of 114.48-fold. Treatment with 50, 100, and 200 µg/mL RRT extract significantly reversed this effect ( $P < 0.001$ ). This suggests that UVB exposure diminishes tissue remodeling and contributes to skin aging.

### Accumulation of inflammatory factors induces senescence in HFF

UVB radiation has been established to induce senescence in keratinocytes; however, the direct role of inflammatory factors in senescence remains uncertain or potentially indirect. Dermis aging is a significant aspect of the skin aging process; thus, we aimed to investigate the impact of inflammatory factors on HFF by conducting experiments as shown in Fig. 5a. We analyzed the gene expression levels of MMP1 and MMP3

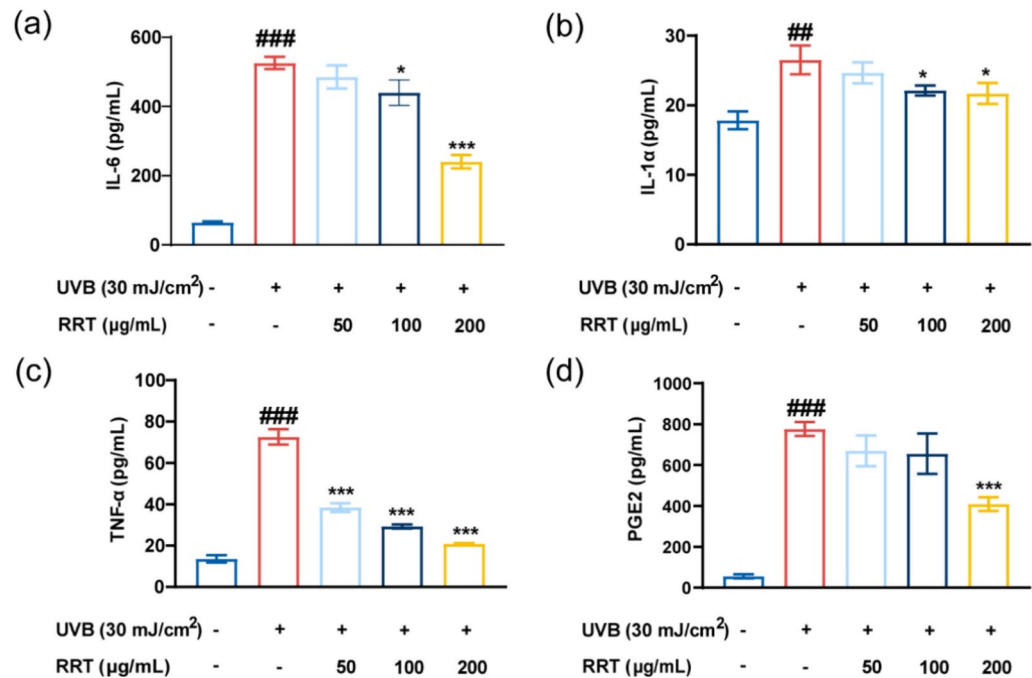


**Fig. 3.** Results of secretion levels of inflammatory factors. (a) IL-1α, (b) IL-6, (c) TNF-α, and (d) PGE2 in supernatants. Statistical analysis involved one-way ANOVA and paired two-tailed t-tests, with significance denoted as <sup>###</sup> $P < 0.001$ , <sup>##</sup> $P < 0.01$ , <sup>\*</sup> $P < 0.05$  relative to the control group, and <sup>\*\*\*</sup> $P < 0.001$ , <sup>\*\*</sup> $P < 0.01$ , <sup>\*</sup> $P < 0.05$  relative to the control group.

(proteases involved in matrix degradation), COL1A1 (associated with collagen synthesis), and TGF-β1 and Smad2 (involved in tissue repair and regeneration) over incubation periods of 1, 2, 4, 6, and 8 d. To examine the effect of incubation duration in the inflammatory medium on cellular senescence, a heatmap of the results was generated, as illustrated in Fig. 5b. The expression levels of MMP1 and MMP3 exhibited an upward trend with prolonged treatment, reaching their maxima on the 6th day. By the 8th day, the upregulation of both genes began to decrease. In contrast, COL1A1 expression was relatively low during the early stages (days 1 and 2) but progressively increased over time, peaking on the 8th day. The expression levels of TGF-β1 and Smad2 consistently increased at all time points. Furthermore, as illustrated in Fig. 5c, the gene expression levels of MMP1, MMP3, TGF-β1, and Smad2 exhibited significant changes compared to the untreated group when exposed to the inflammatory medium within the 1st day of incubation, whereas the changes in COL1A1 were less pronounced. After the 2nd day, all five genes showed significant changes in expression. These experimental results demonstrate the significant senescent effect of inflammatory factors on HFF and underscore the significant impact of prolonged inflammatory factor accumulation on cellular senescence.

### Inflammatory factors damage mitochondrial function

As shown in Fig. 6a, there was a marked increase in green fluorescence and a slight decrease in red fluorescence in HFF after treatment with inflammatory media, suggesting a significant reduction in MMP. Further examination of the flow cytometry data presented in Fig. 6b demonstrates a decrease in red fluorescence from 69.3 to 41.7%, whereas the proportion of green fluorescence increased from 29.5 to 56.0%. This shift corresponded to a 68.47% decrease in mitochondrial membrane potential (MMP). In addition, as shown in Fig. 6c, following stimulation with inflammatory factors, mtROS levels in HFF exhibited a significantly increased from 3407 to 3674. Moreover, as shown in Fig. 6d, the total ROS levels in HFF increased by 235.9% under the influence of inflammatory factors, highlighting the significant regulatory impact of inflammatory factors on cellular oxidative stress responses. In summary, inflammatory factors effectively augment ROS levels and mtROS activity, leading to excessive accumulation of ROS that cannot be adequately cleared and concurrently reduce MMP.

### RRT extract restores inflammatory factors induced HFF senescence

Given the anti-inflammatory properties of the RRT extract and the senescence processes induced by inflammatory factors, it is imperative to further investigate the anti-inflammatory potential of the RRT extract. Enhanced β-Gal activity is recognized as a hallmark of cellular senescence. As illustrated in Fig. 7a, the control group exhibits cells with normal morphology and weak staining. In contrast, the model group demonstrates a significant increase in staining intensity, characterized by a pronounced blue coloration (as indicated by the red arrows). The deeper blue hue signifies elevated β-Gal activity, which correlates with a higher prevalence of senescent cells. This observation implies that the cells may have experienced senescence or stress. Notably, as the concentration of RRT increases (50, 100, and 200 μg/mL), there is a progressive decrease in staining intensity. This finding suggests that RRT may mitigate cell senescence or stress within the model group. Furthermore,



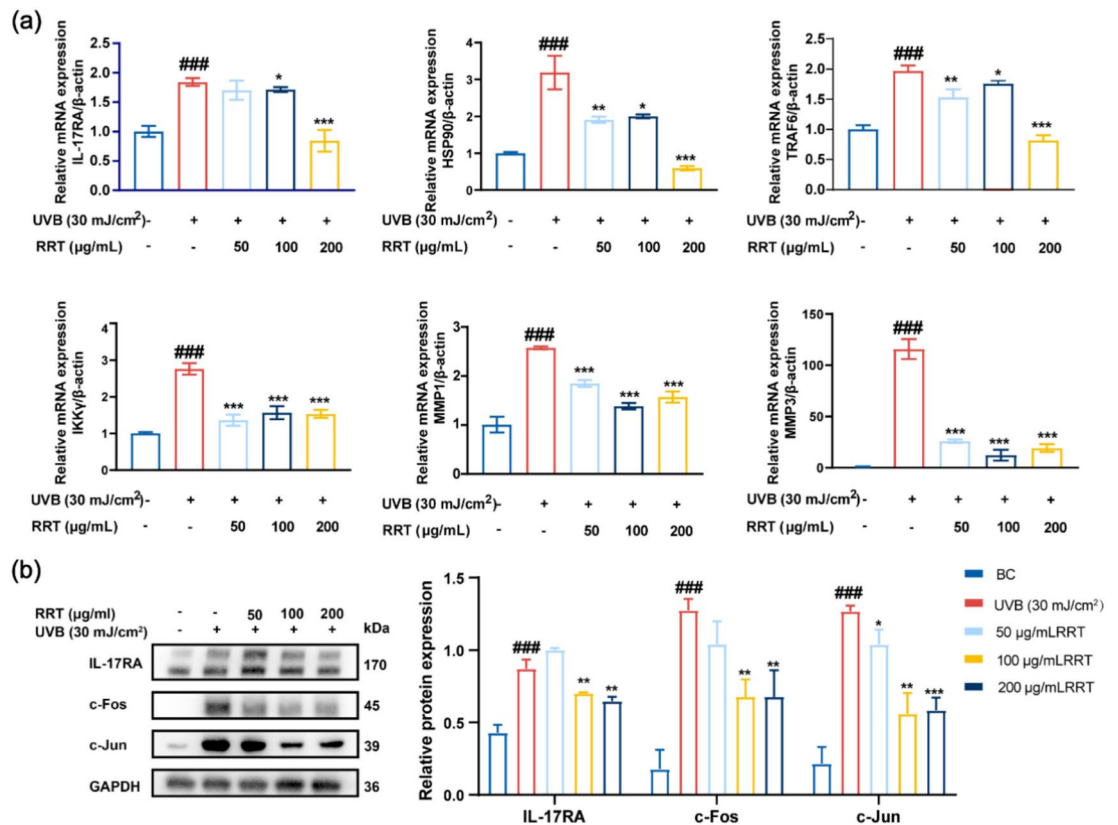


**Fig. 4.** RRT extract suppresses IL-17 pathway in UVB-induced keratinocytes. **(a)** Relative mRNA expression levels of IL-17RA, HSP90, TRAF6, IKKγ, MMP1 and MMP3 in keratinocytes. **(b)** Western blot electrophoresis results and relative proteins expression levels of IL-17RA, c-Fos, and c-Jun in keratinocytes. Statistical analysis involved one-way ANOVA and paired two-tailed t-tests, with significance denoted as ### $P < 0.001$ , ## $P < 0.01$ , # $P < 0.05$  relative to the control group, and \*\*\* $P < 0.001$ , \*\* $P < 0.01$ , \* $P < 0.05$  relative to the control group.

quantitative analysis using flow cytometry revealed that treatment with the inflammatory medium increased  $\beta$ -Gal activity by 56.2%. Treatment with RRT extract at 100 and 200  $\mu$ g/mL significantly reduced  $\beta$ -Gal activity ( $P < 0.05$ ), with the 200  $\mu$ g/mL RRT group showing a 20.55% decrease in  $\beta$ -gal activity compared to the model group (Fig. 7b). These findings collectively indicate that RRT extract effectively reduces the increase in  $\beta$ -gal activity induced by inflammatory factors.

Furthermore, the addition of the RRT extract restored the gene expression levels of COL3A1 induced by inflammatory factors (Fig. 7c). As shown in Fig. 7d, 100 and 200  $\mu$ g/mL RRT extract significantly increased the protein expression of COL1A1 ( $P < 0.05$ ), respectively. In addition, protein detection revealed that the inflammatory medium significantly decreased the expression of TGF- $\beta$ 1 and phosphorylated Smad2/3 ( $P < 0.05$ ). However, concentrations of 50, 100, and 200  $\mu$ g/mL of RRT extract all exhibited significant downregulation effects on TGF- $\beta$ 1 and smad2/3 proteins ( $P < 0.05$ ). This suggests that the inflammatory medium suppresses inflammaging by inhibiting the TGF- $\beta$ 1-Smad2/3 signaling pathway, whereas RRT extract demonstrates anti-inflammaging effects by activating this pathway. The SASP refers to a series of factors, inflammatory factors, and extracellular matrix proteins produced and secreted by senescent cells<sup>21</sup>. Further genetic tests showed that RRT extract effectively reduces the secretion of inflammatory factors IL-1 $\alpha$ , IL-6, MMP1, MMP3, CXCL1 and TGF- $\beta$ 1 through senescence cells (Fig. 7e). In conclusion, RRT extract exerts anti-inflammaging effects by regulating the TGF- $\beta$ 1-Smad2/3 signaling pathway, activating collagenase activity, inhibiting  $\beta$ -Gal activity, and reducing SASP production.

## Discussion

UV radiation, environmental pollution, and other external stimuli can trigger skin inflammation, accelerate the process of inflammaging and create a detrimental cycle of inflammation and senescence<sup>22,23</sup>. Rich in polyphenolic compounds, RRT extracts are recognized for their potent antioxidant and anti-inflammatory properties. However, the precise mechanism of action of RRT extract in combating skin inflammaging remains elusive. Therefore, investigating the role of inflammatory factors in senescence and exploring the anti-inflammatory efficacy of the RRT extract is crucial. In our study the skin microenvironment was simulated demonstrating that UVB-induced keratinocyte damage release inflammatory factors which effectively promote HFF inflammaging. Notably, the RRT extract exerted anti-inflammatory effects by inhibiting the activation of the IL-17 signaling

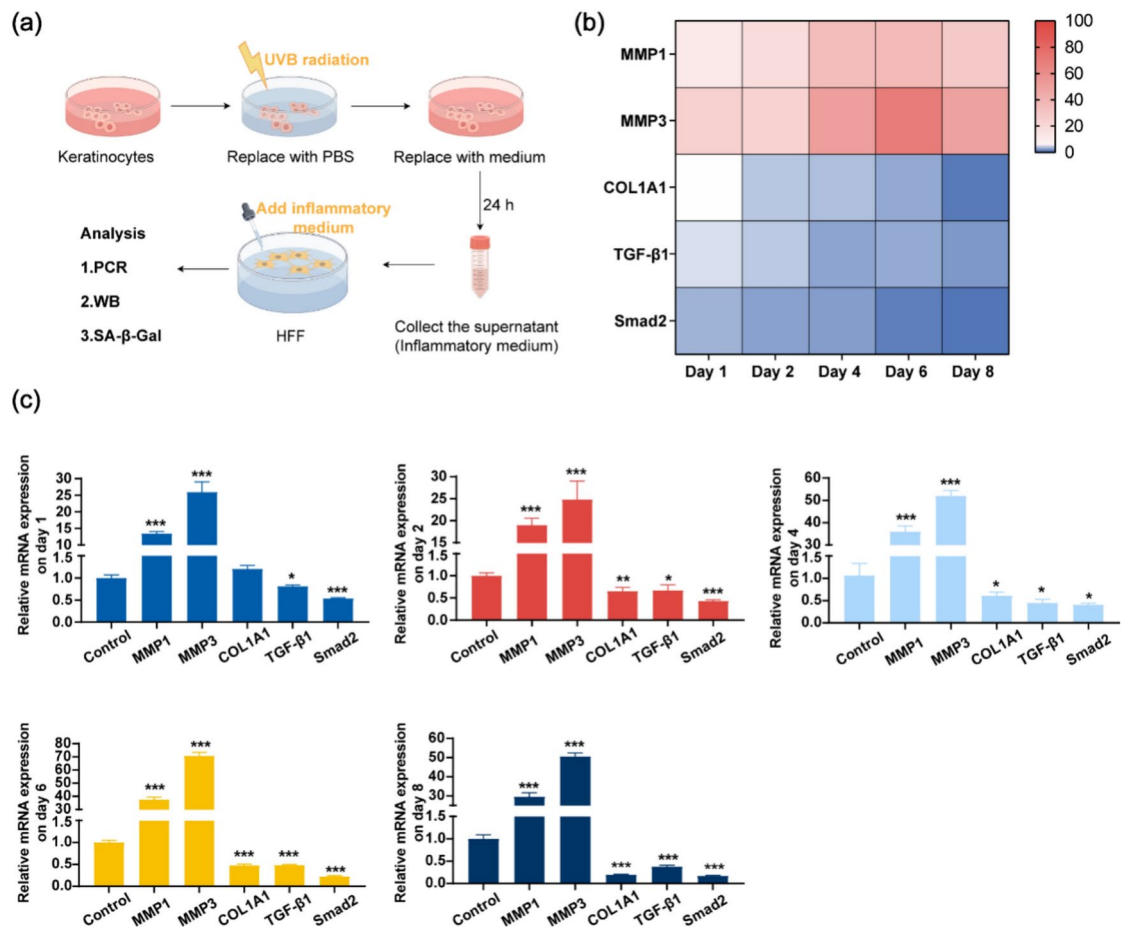


**Fig. 5.** Accumulation of inflammatory factors induces senescence in HFF. (a) Flowchart showing how keratinocyte-secreted inflammatory factors interact with HFF. (b) Heat maps depicting genes expression levels of senescence markers at different time points. (c) Relative MMP1, MMP3, COL1A1, TGF-β1, and Smad2 mRNA levels in HFF on days 1, 2, 4, 6, and 8, respectively. Statistical analysis involved one-way ANOVA and paired two-tailed t-tests, with significance denoted as \*\*\* $P < 0.001$ , \*\* $P < 0.01$ , and \* $P < 0.05$  relative to the control group.

pathway. Consequently, RRT extract has emerged as a potential therapeutic candidate for anti-inflammatory effects.

In this study, we examined the anti-inflammatory mechanisms of the RRT extract through gene and protein analyses. Following UVB stimulation, keratinocytes exhibited significant upregulation of IL-17RA signaling-related genes, which were markedly downregulated following treatment with the RRT extract. In addition, the RRT extract significantly suppressed IL-17RA protein expression and downstream signaling pathways in keratinocytes. Moreover, RRT extract effectively reduced the secretion of inflammatory factors such as IL-6 and TNF-α, underscoring its capability to modulate inflammatory responses by targeting the IL-17 signaling pathway. Previous studies on Gingerenone A demonstrated similar anti-inflammatory effects by inhibiting IL-17RA protein expression and reducing the expression of various inflammatory factors<sup>24</sup>. Moreover, research has indicated the inhibition of the IL-17 signaling pathway can effectively delay aging<sup>25</sup>. Our findings indicate that the RRT extract effectively inhibits MMP1 gene expression, which is responsible for the degradation of major structural and elastic proteins within cells, contributing to skin wrinkles and laxity<sup>26</sup>. This further underscores its potential to achieve anti-inflammatory effects through suppression of the IL-17 pathway.

Furthermore, the impact of keratinocyte-derived inflammatory factors on the surrounding cells was explored in our study, revealing their role in promoting HFF senescence. This underscores the role of keratinocytes as crucial signal transmitters in the skin, influencing surrounding cellular function and metabolic status through paracrine effects. Previous research has illustrated how keratinocytes release factors that influence surrounding cell functions such as melanogenesis in B16F10 cells<sup>27</sup>. Our findings emphasize how the inflammatory response in keratinocytes affects the senescence of neighboring cells. The effects of inflammatory factors released by keratinocytes on HFF senescence were investigated using a custom-made inflammaging model. Guo et al. showed that the inflammatory factor TNF-α induces senescence in HUVECs, resulting in increased β-Gal activity and P21 expression<sup>28</sup>. In addition, Yue et al. treated thymic epithelial cells with 10 ng/mL of TNF-α and 20 ng/mL of IL-6, and showed that these inflammatory factors significantly promoted cellular senescence<sup>29</sup>.

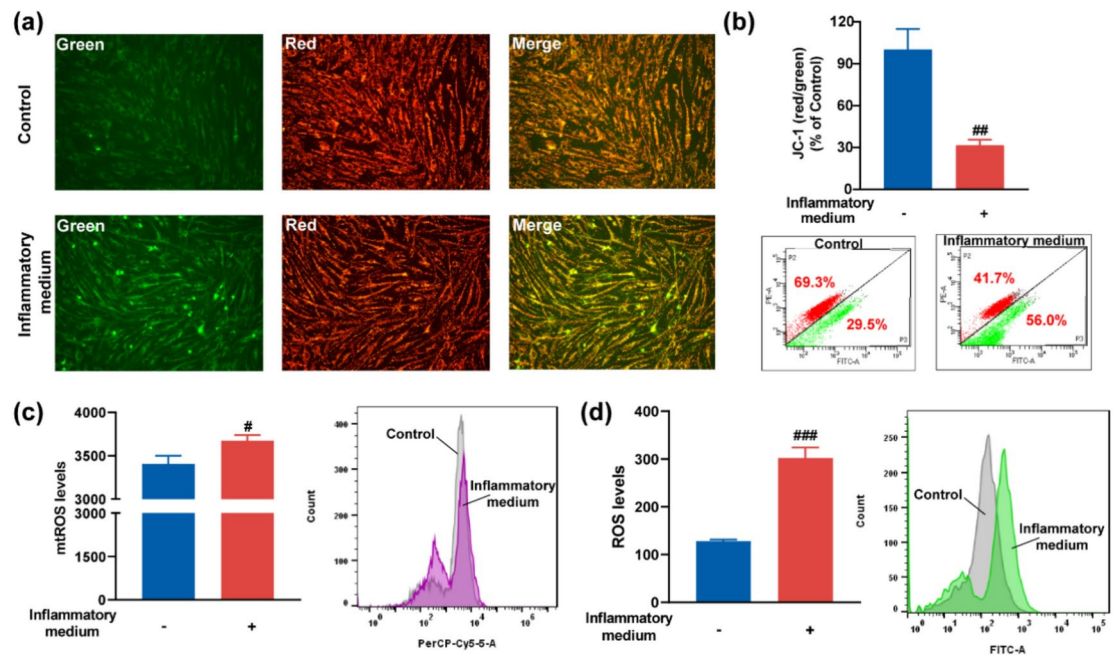


**Fig. 6.** Inflammatory factors damage mitochondrial function. **(a)** Fluorescence imaging of HFF stained with JC-1 (magnification:  $\times 20$ ): red indicates aggregates in healthy mitochondria, while green marks cytoplasmic monomers, reflecting MMP loss. **(b)** JC-1 analysis in HFF by flow cytometry. **(c)** Measurement of mtROS levels in HFF cells using flow cytometry. **(d)** Evaluation of total ROS levels in HFF by flow cytometry. Statistical analysis involved one-way ANOVA and paired two-tailed t-tests, with significance denoted as ### $P < 0.001$ , ## $P < 0.01$ , and # $P < 0.05$  relative to the control group.

Notably, significant signs of senescence in HFF were observed as early as the 1st day after treatment with low concentrations of inflammatory factors (such as PGE2 and IL-6 of  $< 1000$  pg/mL, IL-1 $\alpha$  and TNF- $\alpha$  of  $< 100$  pg/mL) in this study. This could be attributed to the synergistic action of multiple inflammatory factors. Subsequent extended culture revealed that MMP3 peaked on the 6th day before declining, possibly due to self-regulatory responses after cellular damage; however, the cell may self-destroy once the damage is beyond its ability to repair<sup>30</sup>. Dihydrotestosterone treatment of dermal papilla cells induces mitochondrial ROS accumulation and thus cell senescence<sup>31</sup>. In addition, UVB irradiation of HDFs results in a decreased mitochondrial membrane potential and increased ROS levels, leading to cell senescence<sup>32</sup>. This supports the idea that inflammatory factors cause cellular senescence by affecting mitochondrial function.

In terms of exploring the mechanism of the anti-inflammatory activity of RRT extract, RRT extract only interfered with keratinocytes before UVB irradiation. This experimental design highlights the potential of the RRT extract in regulating skin physiology. Our findings revealed a positive correlation between the anti-aging effects of RRT in HFF and the reduced levels of inflammatory factors in keratinocytes, confirming the critical role of inflammation in cell senescence.  $\beta$ -Gal activity, a widely used senescence marker, exhibits increased activity post-multiple cell divisions<sup>33</sup>. Liu et al. reported that flavones derived from *Prinsepia utilis* Royle seed residue inhibit  $\beta$ -Gal activity to combat replicative aging<sup>34</sup>, suggesting RRT extract may preserve cellular function by delaying replicative aging processes. Moreover, our study highlighted the promotion of COL1A1 expression by RRT, a vital skin structural protein that is crucial for maintaining elasticity and structural integrity<sup>35</sup>. Molecularly, the upregulation of the TGF- $\beta$ 1-Smad2/3 signaling pathway indicated the potential of RRT in promoting skin tissue repair and regeneration by enhancing cell proliferation and matrix synthesis<sup>36</sup>. Furthermore, RRT extract treatment led to a reduction in SASP factors in HFF, which are pivotal for cellular and tissue inflammatory responses. In summary, our study revealed the potential of RRT in skin anti-aging, particularly through mechanisms mitigating replicative, tissue-, stress-induced, and inflammation-related aging, providing foundational insights for novel anti-aging strategies.

## Conclusions

UVB radiation downregulates the IL-17 signaling pathway, resulting in the release of inflammatory factors TNF- $\alpha$ , IL-6, IL-1 $\alpha$ , and PGE2, which induce a robust inflammatory response in keratinocytes. This cascade upregulates the expression of MMP1 and MMP3, thereby contributing to cell aging. These inflammatory factors exert paracrine effects on HFF, leading to decreased mitochondrial membrane potential and increased mitochondrial ROS levels. In addition, these inflammatory factors downregulate the TGF- $\beta$ 1-Smad2/3 signaling pathway, increase  $\beta$ -Gal activity, and decrease expression of COL1A1 and COL3A1, thereby contributing to HFF aging. Senescent cells further accelerate the aging process by secreting the SASP. The RRT extract suppressed

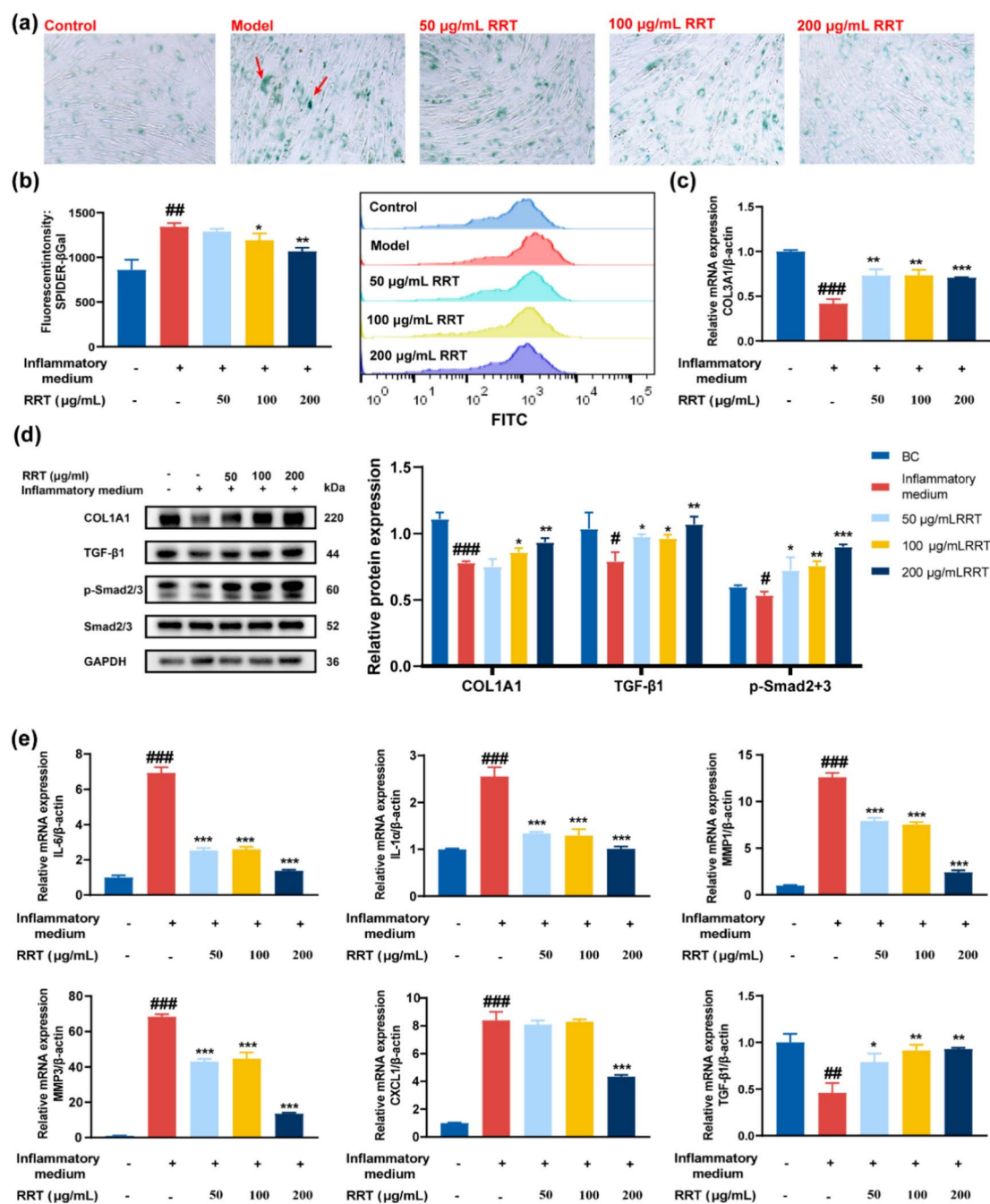


**Fig. 7.** RRT extract restores inflammatory factors induced HFF senescence. (a) Representative images of β-Gal staining (magnification: ×20). (b) Flow cytometry analysis of β-Gal activity in HFF. (c) Relative COL3A1 mRNA levels in HFF. (d) Western blot electrophoresis results and relative COL1A1, TGF-β1, and Smad2/3 proteins levels in HFF. (e) The relative mRNA expression levels of SASP factors, including IL-6, IL-1α, MMP1, MMP3, CXCL1, and TGF-β1, in HFF. Statistical analysis involved one-way ANOVA and paired two-tailed t-tests, with significance denoted as <sup>###</sup> $P < 0.001$ , <sup>##</sup> $P < 0.01$ , and <sup>#</sup> $P < 0.05$  relative to the control group, and <sup>\*\*\*</sup> $P < 0.001$ , <sup>\*\*</sup> $P < 0.01$ , and <sup>\*</sup> $P < 0.05$  relative to the inflammation medium group.

inflammatory responses by downregulating the IL-17 pathway in keratinocytes, thereby mitigating their paracrine effects and achieving anti-inflammaging effects in HFF. This mechanism is summarized in Fig. 8.

## Materials and methods

### Plant materials

In October 2023, *Rosa roxburghii* Tratt. (RRT) was collected from Kunming, Yunnan Province, China, with permission from the Kunming Institute of Botany (permission No. 2023-10), in compliance with relevant institutional, national, and international guidelines and legislation. The plant material was identified and



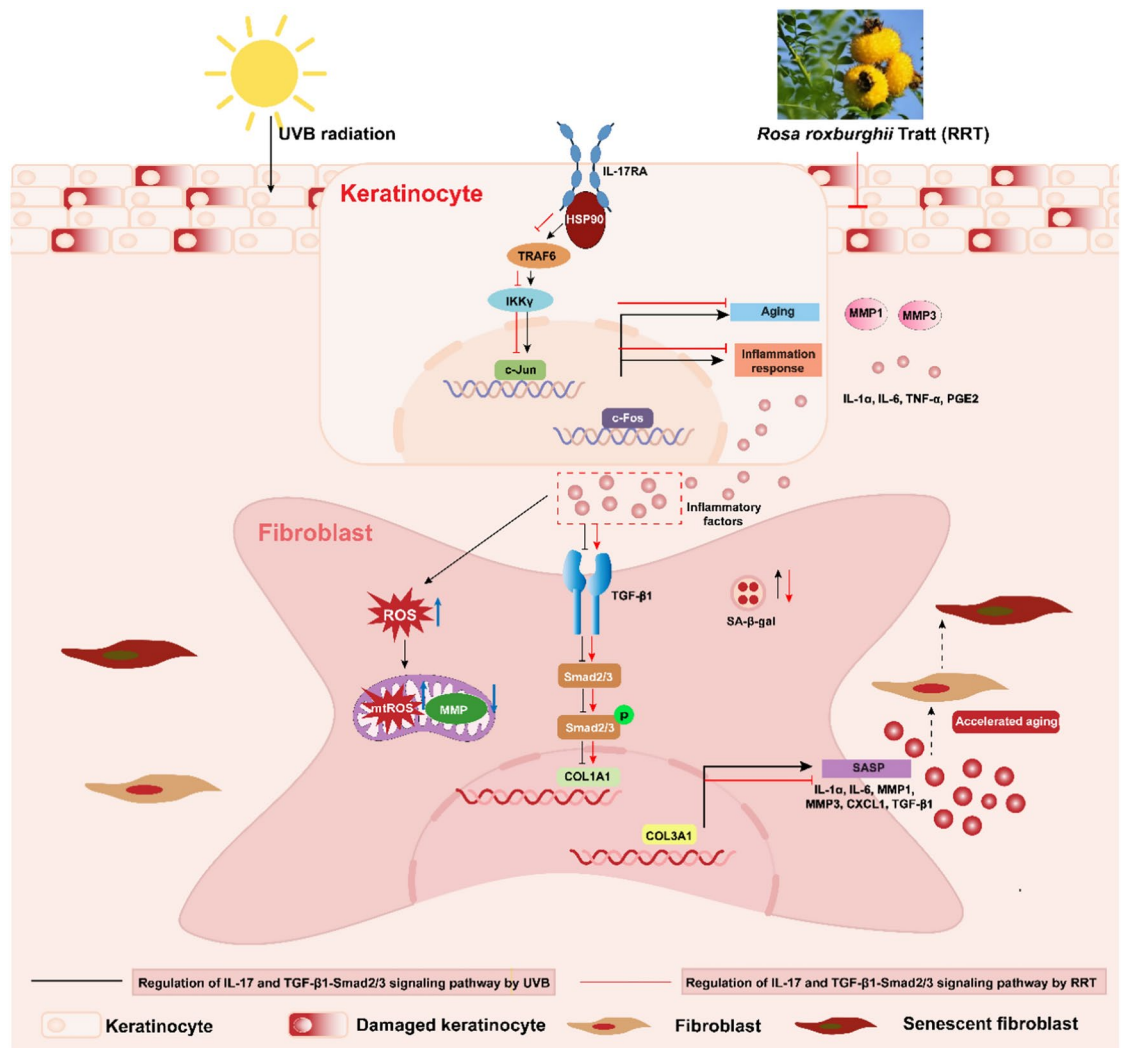


**Fig. 8.** Schematic illustration of molecular pathways in UVB-induced keratinocyte inflammation and the senescence-promoting effects of inflammatory factors on HFE.

authenticated by Professor Haiyang Liu at the Kunming Institute of Botany. A voucher specimen (No. 20231008) has been deposited at the herbarium of the Botany Research Institute, Shanghai Jiyan Bio-Pharmaceutical Development Co., Ltd., Shanghai, China. No endangered or protected species were involved in this study.

### Preparation and chemical composition analysis of the RRT fruit extract

The dried and cleaned RRT were powdered using a grinder and sieved. RRT powder (100 g) was added to 1000 mL water. The mixture was refluxed at 60 °C for 2 h; this process was repeated once. The combined filtrates were concentrated using low-pressure drying. The concentrated extract was then subjected to freeze-drying, yielding an RRT extract with a mean yield of 50.14% ± 3.41%.

The chemical composition of the RRT fruit extract was analyzed by an Agilent 1290 HPLC system (Agilent, Palo Alto, USA). Separation was performed on an Agilent ZORBAX SB-AQ column (250 mm × 4.6 mm, 5 μm) at 30 °C, with a 10 μL injection volume. The mobile phase consisted of solvent A (water) and solvent B (Acetonitrile), using a gradient elution with the following conditions: 0–6 min, 55% B; 6–20 min, 95% B. The flow rate was set at 0.4 mL/min, and detection was performed at 245 nm, with retention times recorded.

To verify the presence of ascorbic acid in the RRT fruit extract, a standard sample of ascorbic acid was run under identical chromatographic conditions. The retention times of the RRT fruit extract and the ascorbic acid standard were compared to assess the similarity in composition.

### Chemicals

Dulbecco's modified Eagle's medium (DMEM), fetal bovine serum (FBS), and trypsin–EDTA were procured from Gibco (New Zealand). Enzyme-linked immunosorbent assay (ELISA) kits for IL-6, IL-1α, and TNF-α were purchased from Neobioscience (Wuhan, China), whereas the PGE2 kit was obtained from Cayman Chemical (MI, USA). The RNA Purification Kit (K0731) and M-PER mammalian protein extraction reagents were acquired from Thermo Fisher Scientific. The loading buffer and bicinchoninic acid (BCA) protein assay kit were

purchased from Beyotime. The Cell Counting Kit-8 (CCK-8), JC-1 MitoMP Detection Kit (MT09), Mitochondrial Superoxide (mtSOX) Detection Kit (MT14), ROS Assay Kit (R253) and Cell Senescence Detection Kit-SPIDER- $\beta$ Gal (SG03) were purchased from Dojindo Molecular Technologies (Shanghai, China). Antibodies against IL-17RA (ab263908), c-Fos (ab222699), TGF- $\beta$ 1 (ab179695), Smad2/3(ab202445), and p-Smad2/3 (ab254407) were purchased from Abcam. Antibodies against c-Jun (9165T) and COL1A1 (72026T) were purchased from Cell Signaling Technology. GAPDH antibody (10494-1-AP) was obtained from Proteintech (Wuhan, China).

### Cell culture and treatment

Keratinocytes and HFF cell lines, sourced from the Cell Bank of the Chinese Academy of Sciences, were cultivated in DMEM containing 10% FBS and 1% penicillin–streptomycin. The cells were incubated under 5% CO<sub>2</sub> at 37 °C in a humidified environment.

### Determination of cell viability using the CCK-8 assay

Cell viability was determined via the CCK-8 method. Briefly, cells were allowed to adhere and subsequently treated with varying concentrations of RRT extract. After 24 h of incubation, each well received 100  $\mu$ L of 10% CCK-8 in DMEM and was incubated for another 2 h at 37 °C. Cell viability was measured by recording absorbance at 450 nm with a Thermo Scientific Multiskan Sky microplate spectrophotometer.

### UVB exposure and RRT extract intervention method

Keratinocytes were irradiated with UVB using a HOPE-MED 8130GT system (Tianjin, China) in line with standard protocols<sup>36</sup>. At 70% confluence, cells were incubated with RRT extract in DMEM with 10% FBS for 2 h. Subsequently, RRT extract in PBS was introduced, and cells were subjected to UVB irradiation at 30 mJ/cm<sup>2</sup>. Post-UVB exposure, PBS was replaced with DMEM containing 10% FBS, and the cell morphology and viability were assessed after 24 h.

### ELISA assay

Supernatants from each experimental group were collected and centrifuged at 10,000 $\times$ g for 10 min. IL-6, TNF- $\alpha$ , IL-1 $\alpha$ , and PGE2 levels were then quantified using ELISA kits, following the manufacturer's protocols.

### Reverse transcription-quantitative polymerase chain reaction (RT-qPCR) assay

Following a previously reported method<sup>37</sup>, total mRNA was extracted using an mRNA purification kit following the manufacturer's protocol, and subsequently transcribed into cDNA. The obtained cDNA was stored at -80 °C before qPCR analysis. Gene expression levels were then quantified using SYBR Green qPCR performed using a LightCycler<sup>®</sup> 480 instrument (Roche, USA). The specific primers used for RT-qPCR are listed in Supplementary Table S1, with ACTINB serving as an internal control.

### Western blot assay

Western blotting was performed in accordance with a previously established protocol<sup>37</sup>. Total proteins were extracted at 4 °C using Mammalian Protein Extraction Reagent, and concentrations were measured with a BCA protein assay kit. Total proteins were extracted at 4 °C using Mammalian Protein Extraction Reagent, and concentrations were measured with a BCA protein assay kit. Proteins were separated by SDS-PAGE and transferred to PVDF membranes, which were blocked with 5% milk powder in TBST at 25 °C for 1 h. Membranes were then incubated with primary antibodies overnight at 4 °C, followed by a 1-h incubation with secondary antibodies at 25 °C. Protein bands were visualized using an electrochemiluminescence system (Tanon Life Sciences) and analyzed with ImageJ software.

### Construction of inflammaging model

Following the Method described in "UVB exposure and RRT extract intervention method" section, the keratinocytes were exposed to UVB radiation. After 24 h, the supernatant enriched with inflammatory factors (referred to as the inflammatory medium) was centrifuged and collected.

To induce senescence, HFFs were treated with freshly prepared inflammatory medium. Specifically, at the beginning of the experiment (Day 0), cells were incubated with inflammatory medium. Thereafter, the inflammatory medium was replaced with newly prepared fresh medium every 2 days (e.g., on Day 2, Day 4, and Day 6) throughout the incubation period. The experiment was terminated at the designated time points (1, 2, 4, 6, and 8 days), at which cells were harvested for analysis. This process ensured that the cells were continuously exposed to active inflammatory factors during the entire treatment period. Finally, the expression levels of senescence markers in HFF were analyzed to confirm the successful construction of the inflammaging model.

### Mitochondrial membrane potential (MMP), mitochondrial reactive oxygen species (mtROS) and ROS level detection

HFF were cultured in an inflammatory medium for a duration of 4 d. Following this, the JC-1 kit was used to measure MMP, whereas the mtSOX kit was used to detect mtROS levels. In addition, an ROS kit was used to evaluate overall ROS levels. This assessment was performed using a BD FACSVerse<sup>™</sup> flow cytometer (BD Biosciences, San Jose, CA, USA) and fluorescence microscopy (Olympus Corporation, Japan), adhering to the manufacturer's protocols.

## $\beta$ -galactosidase ( $\beta$ -Gal) activity detection

HFF were incubated in inflammatory medium for 4 d. Subsequently, according to the cell senescence detection kit-SPIDER- $\beta$ -Gal protocol, cells were stained and images were captured using a microscope. Flow cytometry was used to analyze the stained cell samples to quantitatively evaluate intracellular  $\beta$ -Gal activity.

## Statistical analysis

All data are presented as means  $\pm$  SD ( $n \geq 3$ ). The cellular experiments were independently replicated three times. Statistical comparisons between two groups were conducted using a two-sided unpaired t-test, while one-way or two-way ANOVA followed by Tukey's post hoc test was used for multiple group analyses. Statistical significance was defined as  $P < 0.05$ .

## Data availability

All data generated or analysed during this study are available from the corresponding author upon reasonable request.

Received: 14 November 2024; Accepted: 28 February 2025

Published online: 10 March 2025

## References

- Franceschi, C. et al. Inflamm-aging: An evolutionary perspective on immunosenescence. *Ann. N. Y. Acad. Sci.* **908**, 244–254. <https://doi.org/10.1111/j.1749-6632.2000.tb06651.x> (2000).
- Pilkington, S. M., Bulfone-Paus, S., Griffiths, C. E. M. & Watson, R. E. B. Inflammaging and the skin. *J. Investig. Dermatol.* **141**, 1087–1095. <https://doi.org/10.1016/j.jid.2020.11.006> (2021).
- Salvioli, S. et al. Immune system, cell senescence, aging and longevity-inflamm-aging reappraised. *Curr. Pharm. Des.* **19**, 1675–1679 (2013).
- Lopez-Otin, C., Blasco, M. A., Partridge, L., Serrano, M. & Kroemer, G. Hallmarks of aging: An expanding universe. *Cell* **186**, 243–278. <https://doi.org/10.1016/j.cell.2022.11.001> (2023).
- Wiggins, K. A. et al. IL-1 $\alpha$  cleavage by inflammatory caspases of the noncanonical inflammasome controls the senescence-associated secretory phenotype. *Aging Cell* **18**, e12946. <https://doi.org/10.1111/acel.12946> (2019).
- Welzel, J., Lankenau, E., Birngruber, R. & Engelhardt, R. Optical coherence tomography of the human skin. *J. Am. Acad. Dermatol.* **37**, 958–963. [https://doi.org/10.1016/s0190-9622\(97\)70072-0](https://doi.org/10.1016/s0190-9622(97)70072-0) (1997).
- Yuan, M. et al. Hyaluronan-modified transfersomes based hydrogel for enhanced transdermal delivery of indomethacin. *Drug Deliv.* **29**, 1232–1242. <https://doi.org/10.1080/10717544.2022.2053761> (2022).
- Lee, H., Kong, G., Park, J. & Park, J. The potential inhibitory effect of ginsenoside Rh2 on mitophagy in UV-irradiated human dermal fibroblasts. *J. Ginseng Res.* **46**, 646–656. <https://doi.org/10.1016/j.jgr.2022.02.001> (2022).
- Qiang, L. et al. Autophagy gene ATG7 regulates ultraviolet radiation-induced inflammation and skin tumorigenesis. *Autophagy* **13**, 2086–2103. <https://doi.org/10.1080/15548627.2017.1380757> (2017).
- Hegedüs, C. et al. Cyclobutane pyrimidine dimers from UVB exposure induce a hypermetabolic state in keratinocytes via mitochondrial oxidative stress. *Redox Biol.* **38**, 101808. <https://doi.org/10.1016/j.redox.2020.101808> (2021).
- Lu, P. H. et al. Spleen tyrosine kinase regulates keratinocyte inflammasome activation and skin inflammation induced by UVB irradiation. *Free Radic. Biol. Med.* **180**, 121–133. <https://doi.org/10.1016/j.freeradbiomed.2022.01.004> (2022).
- Ruan, X. et al. Mechanism of Dayuanyin in the treatment of coronavirus disease 2019 based on network pharmacology and molecular docking. *Chin. Med.* **15**, 62. <https://doi.org/10.1186/s13020-020-00346-6> (2020).
- Johnston, L. A., Nagalla, R. R., Li, M. & Whitley, S. K. IL-17 control of cutaneous immune homeostasis. *J. Investig. Dermatol.* **144**, 1208–1216. <https://doi.org/10.1016/j.jid.2023.11.016> (2024).
- Wang, C. et al. IL-17 induced NOTCH1 activation in oligodendrocyte progenitor cells enhances proliferation and inflammatory gene expression. *Nat. Commun.* **8**, 15508. <https://doi.org/10.1038/ncomms15508> (2017).
- Sultana, R., Parveen, A., Kang, M. C., Hong, S. M. & Kim, S. Y. Glyoxal-derived advanced glycation end products (GO-AGEs) with UVB critically induce skin inflammaging: in vitro and in silico approaches. *Sci. Rep.* **14**, 1843. <https://doi.org/10.1038/s41598-024-52037-z> (2024).
- Xu, D. et al. The synergistic action of phosphate and interleukin-6 enhances senescence-associated calcification in vascular smooth muscle cells depending on p53. *Mech. Ageing Dev.* **182**, 111124. <https://doi.org/10.1016/j.mad.2019.111124> (2019).
- Huang, Y., Chen, X., Liu, X., Lin, C. & Wang, Y. The coumarin component isofraxidin targets the G-protein-coupled receptor S1PR1 to modulate IL-17 signaling and alleviate ulcerative colitis. *Int. Immunopharmacol.* **131**, 111814. <https://doi.org/10.1016/j.intimp.2024.111814> (2024).
- Wang, L. et al. Component analysis and anti-pulmonary fibrosis effects of *Rosa sterilis* juice. *Food Funct.* **13**, 12915–12924. <https://doi.org/10.1039/d2fo02758e> (2022).
- Cheng, L., Liu, J., Wang, Q., Hu, H. & Zhou, L. The protective effect of a human umbilical cord mesenchymal stem cell supernatant on UVB-induced skin photodamage. *Cells* **13**, 156. <https://doi.org/10.3390/cells13020156> (2024).
- Xu, S. J. et al. Flavonoids of *Rosa roxburghii* Tratt offers protection against radiation induced apoptosis and inflammation in mouse thymus. *Apoptosis* **23**, 470–483. <https://doi.org/10.1007/s10495-018-1466-7> (2018).
- Saul, D. et al. A new gene set identifies senescent cells and predicts senescence-associated pathways across tissues. *Nat. Commun.* **13**, 4827. <https://doi.org/10.1038/s41467-022-32552-1> (2022).
- Gu, Y., Han, J., Jiang, C. & Zhang, Y. Biomarkers, oxidative stress and autophagy in skin aging. *Ageing Res. Rev.* **59**, 101036. <https://doi.org/10.1016/j.arr.2020.101036> (2020).
- Li, X. et al. Inflammation and aging: signaling pathways and intervention therapies. *Signal Transduct. Target. Ther.* **8**, 239. <https://doi.org/10.1038/s41392-023-01502-8> (2023).
- Liang, J. et al. Gingerenone A attenuates ulcerative colitis via targeting IL-17RA to inhibit inflammation and restore intestinal barrier function. *Adv. Sci.* **11**, e2400206. <https://doi.org/10.1002/adv.202400206> (2024).
- Solá, P. et al. Targeting lymphoid-derived IL-17 signaling to delay skin aging. *Nat. Aging* **3**, 688–704. <https://doi.org/10.1038/s43587-023-00431-z> (2023).
- Budden, T. et al. Ultraviolet light-induced collagen degradation inhibits melanoma invasion. *Nat. Commun.* **12**, 2742. <https://doi.org/10.1038/s41467-021-22953-z> (2021).
- Hseu, Y. C. et al. The in vitro and in vivo depigmenting activity of pterostilbene through induction of autophagy in melanocytes and inhibition of UVA-irradiated  $\alpha$ -MSH in keratinocytes via Nrf2-mediated antioxidant pathways. *Redox Biol.* **44**, 102007. <https://doi.org/10.1016/j.redox.2021.102007> (2021).

28. Guo, F., Wu, R. & Xu, J. Salicin prevents TNF- $\alpha$ -induced cellular senescence in human umbilical vein endothelial cells (HUVECs). *Artif. Cell. Nanomed. B* **47**, 2618–2623. <https://doi.org/10.1080/21691401.2019.1629949> (2019).
29. Yue, S., Zheng, X. & Zheng, Y. Cell-type-specific role of lamin-B1 in thymus development and its inflammation-driven reduction in thymus aging. *Aging Cell* **18**, e129652. <https://doi.org/10.1111/acel.12952> (2019).
30. Elmore, S. Apoptosis: A review of programmed cell death. *Toxicol. Pathol.* **35**, 495–516. <https://doi.org/10.1080/01926230701320337> (2007).
31. Jung, Y. H. et al. Cyanidin 3-O-arabinoside suppresses DHT-induced dermal papilla cell senescence by modulating p38-dependent ER-mitochondria contacts. *J. Biomed. Sci.* **29**, 17. <https://doi.org/10.1186/s12929-022-00800-7> (2022).
32. Guerrero-Navarro, L., Jansen-Durr, P. & Cavinato, M. Synergistic interplay of UV radiation and urban particulate matter induces impairment of autophagy and alters cellular fate in senescence-prone human dermal fibroblasts. *Aging Cell* **23**, e14086. <https://doi.org/10.1111/acel.14086> (2024).
33. Dimri, G. P. et al. A biomarker that identifies senescent human cells in culture and in aging skin in vivo. *PNAS* **92**, 9363–9367. <https://doi.org/10.1073/pnas.92.20.9363> (1995).
34. Liu, J. et al. A study on the anti-senescent effects of flavones derived from *Prinsepia utilis* Royle seed residue. *J. Ethnopharmacol.* **328**, 118021. <https://doi.org/10.1016/j.jep.2024.118021> (2024).
35. Péterszegi, G., Andrés, E., Molinari, J., Ravelojaona, V. & Robert, L. Effect of cellular aging on collagen biosynthesis: I. Methodological considerations and pharmacological applications. *Arch. Gerontol. Geriatr.* **47**, 356–367. <https://doi.org/10.1016/j.archger.2007.08.019> (2008).
36. Qu, L., Wang, F. & Chen, Y. Protective effect and mechanism research of *Phyllanthus emblica* Linn. fruit extract on UV-induced photodamage in keratinocytes. *Photochem. Photobiol. Sci.* **22**, 1945–1959. <https://doi.org/10.1007/s43630-023-00423-3> (2023).
37. Chen, Y., Zhang, S. & Qu, L. The protective effect of *Artemisia capillaris* Thunb. extract against UVB-induced apoptosis and inflammation through inhibiting the cGAS/STING pathway. *J. Photochem. Photobiol. B* **258**, 112989. <https://doi.org/10.1016/j.jphoto.2024.112989> (2024).

## Acknowledgements

The authors acknowledge the support provided by the Independent Research Fund of the Yunnan Characteristic Plant Extraction Laboratory (Grants 2022YKZY004 and 2023YKZY004).

## Author contributions

All authors contributed to the manuscript. Conceptualization: S.Z. and Y.C.; Writing—original draft, methodology, visualization, validation, investigation, software, formal analysis, data curation: S.Z.; Writing—review and editing, resources, and supervision: Y.C. and L.Q.; funding acquisition, and project administration: L.Q.

## Declarations

### Competing interests

The authors declare no competing interests.

### Additional information

**Supplementary Information** The online version contains supplementary material available at <https://doi.org/10.1038/s41598-025-92559-8>.

**Correspondence** and requests for materials should be addressed to L.Q.

**Reprints and permissions information** is available at [www.nature.com/reprints](http://www.nature.com/reprints).

**Publisher's note** Springer Nature remains neutral with regard to jurisdictional claims in published maps and institutional affiliations.

**Open Access** This article is licensed under a Creative Commons Attribution-NonCommercial-NoDerivatives 4.0 International License, which permits any non-commercial use, sharing, distribution and reproduction in any medium or format, as long as you give appropriate credit to the original author(s) and the source, provide a link to the Creative Commons licence, and indicate if you modified the licensed material. You do not have permission under this licence to share adapted material derived from this article or parts of it. The images or other third party material in this article are included in the article's Creative Commons licence, unless indicated otherwise in a credit line to the material. If material is not included in the article's Creative Commons licence and your intended use is not permitted by statutory regulation or exceeds the permitted use, you will need to obtain permission directly from the copyright holder. To view a copy of this licence, visit <http://creativecommons.org/licenses/by-nc-nd/4.0/>.

© The Author(s) 2025